one in Scheme III is in better agreement with the results presented.

In conclusion, it was shown that the redox properties of a triplet sensitizer are crucial to Chl*a* singlet state formation. The excitation yield of 0.03 measured in the benzophenone/Chl*a* system indicates a rather efficient process when one takes into account the spin-forbidden nature of the process and the absence of heavy atoms.

The fact that in the excitation of Chl*a* to its singlet state by a triplet sensitizer the redox properties of the latter are important has to be considered when this molecule is used to detect enzymatically generated triplet species. In the case of the operation of the mechanism outlined in Scheme III, the charge or electron-transfer of an acceptor primarily excited by a triplet molecule could be important in the interaction of enzymatically generated triplet species with biomolecules, where processes could be triggered in which an energy transfer would be coupled to electron transfer.

Acknowledgments. Thanks are due to Dr. F. Hartstock for the measurement of the reduction potentials of the different sensitizers, to Mr. S. E. Sugamori for technical assistance, and to Dr. L. J. Johnston for her help in the early stages of this work.

SF_6-Sensitized Infrared Photodecomposition of $Fe(CO)_5$

Tetsuro Majima,* Tadahiro Ishii,† Yoshiyasu Matsumoto, and Michio Takami

Contribution from the Institute of Physical and Chemical Research, Hirosawa, Wako, Saitama, 351-01, Japan. *Received August 18, 1988*

Abstract: The SF_6-sensitized infrared photodecomposition of $Fe(CO)_5$ induced by a transversely excited atmospheric (TEA) CO_2 laser has been studied. The decomposition of $Fe(CO)_5$ proceeds via sequential decarbonylation after thermal equilibrium is attained through collisional V–V and V–T/R processes. $Fe(CO)_4(PF_3)$ is formed as a dominant product at lower conversion in a mixture of SF_6–$Fe(CO)_5$–PF_3, which indicates that the rate-determining process is the first decarbonylation of excited $Fe(CO)_5$ into $Fe(CO)_4$ and CO, and that $Fe(CO)_4$ is trapped by PF_3 to yield $Fe(CO)_4(PF_3)$. In addition, $Fe(CO)_3(PF_3)_2$, $Fe(CO)_2(PF_3)_3$, and $Fe(CO)(PF_3)_4$ are formed progressively with increasing conversion of $Fe(CO)_5$. These higher PF_3-substituted iron complexes are formed by repeated series of thermal excitation, decarbonylation, and trapping by PF_3. Final products are CO and iron particles, following the shot by shot stoichiometry of $Fe(CO)_5 \rightarrow Fe + 5CO$. The iron particles are found to be γ-iron or austenite, (Fe–C)4F, including 0.75 wt % carbon which has a mean particle size of 80 Å and a face-centered-cubic structure. Variations of the decomposition probability by changing the irradiation parameters are qualitatively explained by changes of kinetic temperature in irradiated volume. The decomposition mechanism in SF_6-sensitized infrared photolysis is compared with those in conventional pyrolysis, infrared multiple-photon decomposition, and UV photolysis.

The photochemistry of transition metal carbonyls continues to be of major interest because of the photocatalytic properties of metal carbonyls. Unsubstituted transition metal carbonyls decompose into coordinatively unsaturated species and carbon monoxide(s) by UV and visible light excitation to electronically excited states. Recently much attention has been focused on the coordinatively unsaturated species in solution[1-4] and also in the gas phase[5-7] because of their catalytic activities. In addition to many photochemical studies of metal carbonyls in the visible and UV region, infrared multiple-photon decomposition (IRMPD) of metal carbonyls such as $Ni(CO)_4$, $Fe(CO)_5$, $Cr(CO)_6$, $Mo(CO)_6$, and $W(CO)_6$ has been studied using a frequency-doubled, transversely excited atmospheric (TEA) CO_2 laser at 5 μm[8] and a p-H_2 Raman laser at 16–17 μm.[9] A TEA CO_2 laser as well as a CW CO_2 laser has also been used to decompose metal carbonyls by IR photosensitized reaction[10-12] and by dielectric breakdown.[13]

Since most of the unsubstituted transition metal carbonyls do not absorb or absorb only weakly in the tunable range of a TEA CO_2 laser, it is necessary to add an infrared photosensitizer. Ideally this should be a substance which absorbs the infrared radiation strongly and transfers a sufficient portion of the absorbed energy to the metal carbonyls for decomposition but does not decompose itself or participate in the reaction sequence. It has been well characterized that SF_6 absorbs strongly in the tunable range of a TEA CO_2 laser but does not decompose at a low laser fluence (ca. 2 J cm^{-2}) because of the relatively high threshold fluence for IRMPD.[14-16] The S–F stretching mode (ν_3) of SF_6, centered at 947 cm^{-1},[17] has an exceptionally high extinction coefficient of 0.2 $Torr^{-1}$ cm^{-1} (5.65×10^{-18} cm^2). In fact, SF_6 has been found to be an excellent infrared photosensitizer for inducing decomposition of $Fe(CO)_5$ with a TEA CO_2 laser in a mixture of SF_6, $Fe(CO)_5$, temperature-monitoring gas, and buffer gas with ca. 100 Torr of total pressure.[11,12]

In the present work we studied the infrared photosensitized decomposition of $Fe(CO)_5$ with an interest in using a TEA CO_2 laser for the generation of coordinatively unsaturated species of metal carbonyls as a catalyst. For such application, it should be clarified how activated $Fe(CO)_5$ decomposes into final products,

† Research Associate from Science University of Tokyo, Kagurazaka, Tokyo 162, Japan.

(1) Geoffroy, G. L.; Wrighton, M. S. *Organometallic Photochemistry*; Academic Press: New York, 1979.
(2) Wrighton, M. S.; Grinley, D. S.; Schroeder, M. A.; Morse, D. L. *Pure Appl. Chem.* **1975**, *41*, 671.
(3) Wrighton, M. S.; Graff, J. L.; Kazlansleas, R. J.; Mitchener, J. C.; Reichel, C. L. *Pure Appl. Chem.* **1982**, *54*, 161.
(4) Whetten, R. L.; Grant, E. R. *J. Am. Chem. Soc.* **1982**, *104*, 4270.
(5) Tumas, W.; Gitlin, B.; Rosan, A. M.; Yardley, J. T. *J. Am. Chem. Soc.* **1982**, *104*, 55.
(6) Whetten, R. L.; Fu, K.-J.; Grant, E. R. *J. Chem. Phys.* **1982**, *77*, 3769.
(7) Miller, M. E.; Grant, E. R. *J. Am. Chem. Soc.* **1984**, *106*, 4635.
(8) Au, M.-K.; Hackett, P. A.; Humphries, M.; John, P. *Appl. Phys. Lett.* **1984**, *B33*, 43.
(9) Majima, T.; Tashiro, H.; Midorikawa, K.; Takami, M. *Chem. Phys. Lett.* **1985**, *121*, 65.
(10) Bristow, N. J.; Moore, B. D.; Poliakoff, M.; Ryott, G. J.; Turner, J. J. *J. Organomet. Chem.* **1984**, *260*, 181.
(11) Smith, G. P.; Laine, R. M. *J. Phys. Chem.* **1981**, *85*, 1620.
(12) Lewis, K. E.; Golden, D. M.; Smith, G. P. *J. Am. Chem. Soc.* **1984**, *106*, 3905.
(13) Langsam, Y.; Ronn, A. M. *Chem. Phys.* **1981**, *54*, 277.
(14) Ambartsumyan, R. V.; Gorohkov, Y. A.; Letohkov, V. S.; Makarov, G. N. *Sov. Phys. JETP* **1975**, *42*, 993.
(15) Lyman, J. L.; Jensen, R. J.; Rinck, J.; Robinson, C. P.; Lockwood, D. *Appl. Phys. Lett.* **1975**, *27*, 87.
(16) Fuss, W.; Cotter, T. P. *Appl. Phys.* **1977**, *12*, 265.
(17) Burak, L.; Houston, P.; Sutton, D. G.; Steinfeld, J. I. *J. Chem. Phys.* **1970**, *53*, 3632.

0002-7863/89/1511-2417$01.50/0

whether decarbonylation occurs stepwise or simultaneously, and what kind of coordinatively unsaturated species are long-lived during the decomposition process. Thus the yield of carbon monoxide (CO) and the consumption of $Fe(CO)_5$ at each laser shot were studied quantitatively as well as the decomposition rate constant as a function of the number of laser pulse, laser fluence, sample pressure, and additive gases. The final solid product was also analyzed chemically. In order to elucidate the coordinatively unsaturated species formed initially, trapping of the species was attempted by adding a large excess of PF_3 to the gas mixture.

Experimental Section

A Lumonics 821 TEA CO_2 laser was operated using a mixture of He, CO_2, and N_2 as flowing gases at a repetition rate of 1 Hz. The laser beam was passed through an aperture of 1.1 cm in diameter, attenuated with KBr disks for fluence dependence studies, and then introduced into an irradiation cell without focusing. The pulse width was 80 ns fwhm with a 1.3-μs tail, with more than 90% of the total energy in the first short spike. More than 95% of the laser energy entered into the cell, and the remaining 5% was reflected into a Genteck joulemeter by using a KBr disk for monitoring the incident laser energy. The transmitted laser energy was also monitored simultaneously by another Genteck joulemeter for measurement of absorbed energy by the sample gas. The laser line was fixed to 10*P*(24) at 940.55 cm^{-1}, which corresponded to the absorption peak of SF_6 at high laser intensity[18] and probably the wavenumber most effective for infrared multiple-photon excitation.

A crossed-type reaction cell used in the present work has a 2.0-cm inner diameter, 10-cm irradiation length, 5-cm long crossed arm for a low-resolution infrared analysis, and 50-cm^3 internal volume (V_{cell}). The cell, equipped with KBr windows, has a cold finger to separate CO from the other condensable gases at −196 °C. The pressure in the cell was monitored by a MKS Baratron (222 BHS) capacitance manometer in the range of 0–10 Torr.

The partial pressure of $Fe(CO)_5$ was estimated from the ν_6 IR absorption peak at 2033.8 cm^{-1} [19] before, during, and after the irradiation. The absorbance at room temperature was measured with a low-resolution infrared spectrometer (JASCO A-102) and a tunable diode laser (Spectra Physics). The partial pressure of CO formed by decomposition of $Fe(CO)_5$ was measured with a tunable diode laser by monitoring infrared absorption of CO ($v = 1 \leftarrow 0$, $P(17) = 2073.26$ cm^{-1}). After irradiation, CO was separated from the rest of condensable gas at −196 °C by means of a Toepler pump, and analyzed with a Shimadzu GC-7A gas chromatograph (column, 3 mm × 3 m Unibeads C 60/80; column temperature, 40 °C; detector, thermal conductivity cell), and then introduced into a NEVA TE-150 quadrupole mass spectrometer to confirm the mass number. The condensed gases were analyzed with the IR spectrometer, the mass spectrometer, and a Shimadzu UV-260 spectrophotometer. When hydrocarbons were used as additives, they were separated from iron carbonyl by passing through a trap cooled to ~−20 to −30 °C and analyzed with a Hitachi 163 gas chromatograph (column, 3 mm × 10 m 10% Sebaconitrile-Uniport 60/80 or 2 mm × 4 m Unicarbon, column temperature, 30 or 50 °C, respectively; detector, flame ionization). When PF_3 was used as an additive gas, SF_6 and PF_3 were separated from $Fe(CO)_5$, $Fe(CO)_{5-x}(PF_3)_x$ (x = 1–4) and $Fe(PF_3)_5$ by fractional distillation at −47 °C by using *m*-xylene refrigerated by liquid nitrogen. The separated gases were analyzed with IR and UV spectrometers, and also with a Hitachi 263-70 gas chromatograph for the latter gas samples (column, 3 mm × 3 m SP-2100 10% Supelcoport 100/120; column temperature, 95 °C; detector, thermal conductivity cell).

The black solid product was characterized by a scanning electron microscope (SEM), a transmission electron microscope (TEM), an ICP atomic emission spectrometer, and an X-ray diffractometer. In order to obtain enough solid product for these analyses, a mixture of SF_6 and $Fe(CO)_5$ was led into a 20-cm long Pyrex cell with 2.8-cm inner diameter at a constant flow rate and total pressure. After irradiation the cell was evacuated for several hours to remove volatile and adsorbed species. The solid was collected by a spatula and the sample for SEM and X-ray diffractometry was prepared under argon atmosphere to avoid exposure to air. For a detailed characterization of the deposition product, conditions were chosen so that the powder formed by the decomposition deposited on Cu disks for SEM and glass slips for X-ray diffractometry.

Reference samples of $Fe(CO)_{5-x}(PF_3)_x$ and $Fe(PF_3)_5$ for gas chromatograph were prepared in the UV–photochemical ligand exchange reaction of $Fe(CO)_5$ by PF_3 with a 400-W mercury high-pressure lamp (Toshiba 400-P).[20] Separation and purification of $Fe(CO)_{5-x}(PF_3)_x$ and $Fe(PF_3)_5$ were carried out by using a gas chromatograph with the column described above. The IR spectra and the gas chromatograph of each purified $Fe(CO)_{5-x}(PF_3)_x$ and $Fe(PF_3)_5$ did not show any detectable impurities. $Fe(CO)_5$ (Strem Chemicals) was distilled in vacuo and degassed by several freeze–pump–thaw cycles with dry ice/methanol to remove trace of CO. It was stored in the dark at −4 °C under an inert gas atmosphere when not in use. SF_6 (Asahi Glass Co.), PF_3 (Japan Oxygen Co.), and other gases (Takachiho Trade Co.) were of the highest purity grades available from the manufacturer and were used without further purification.

Results and Discussion

Products and Stoichiometry. Efficient decomposition of $Fe(CO)_5$ occurred by irradiation of a mixture of SF_6 (1 Torr) and $Fe(CO)_5$ (1 Torr) with an unfocused laser beam of ca. 0.1 J cm^{-2} laser fluence. Only CO was obtained as a volatile product, while a black solid deposited on the entrance window and the cell wall. The solid product was found to be ultrafine particles of metallic iron, characterization of which is described in the following section. No other products were detected by IR spectroscopic, gas chromatographic, and mass spectrometric analyses. On the other hand, SF_6 was recovered in 100% yield even when more than 95% of $Fe(CO)_5$ decomposed. The SF_6 molecule remained unreactive in the presence of a wide variety of additives (0.01–2 Torr) such as Ar, $Fe(CO)_5$, olefins, or PF_3, at a laser fluence of 0.01–0.3 J cm^{-2}. Irradiation of $Fe(CO)_5$ in the absence of SF_6 induces excitation of $Fe(CO)_5$ to lower vibrational levels[21] but does not cause decomposition of $Fe(CO)_5$ at all.

From measurements of the yield of CO and the consumption of $Fe(CO)_5$ by using the gas chromatograph and the low-resolution infrared spectrometer, respectively, the ratio of CO product to the consumed $Fe(CO)_5$ was measured to be 4.7 ± 0.3 after irradiation of 10 laser pulses. This ratio is in good agreement with the stoichiometry

$$Fe(CO)_5 \rightarrow Fe + 5CO \qquad (1)$$

The amounts of stable unsubstituted iron carbonyls such as $Fe_2(CO)_9$ and $Fe(CO)_3(CO)_{12}$ were not detected in the present measurement; the infrared measurements of the deposits on the window and the cell showed no characteristic absorptions by these compounds.

In order to elucidate whether the above stoichiometry follows at each laser shot, the yield of CO and the consumption of $Fe(CO)_5$ were measured as a function of the number of laser pulses with a tunable diode laser and a low-resolution infrared spectrometer, respectively. The pressure of CO increased with an increase in the number of pulses as shown in Figure 1. When X molecules of CO are formed from one $Fe(CO)_5$ molecule, the pressure of CO ([CO]) is expressed by

$$[CO] = X(1 - (1 - d)^N)[Fe(CO)_5]_0 \qquad (2)$$

where d denotes decomposition rate of $Fe(CO)_5$ per pulse, N the number of pulses, and $[Fe(CO)_5]_0$ the initial pressure of $Fe(CO)_5$. Figure 1 shows a comparison of experimental data with eq 2 for X = 4, 5, and 6. The experimental result gives X between 4 and 5 in average but closer to 5 at a small number of laser shots, indicating almost entire decomposition of $Fe(CO)_5$ into iron atom and five CO molecules for each laser shot. The decrease of X for N = 3, 4, and 5, where a substantial quantity of CO has been accumulated in the cell, may be due to the back-reaction between coordinatively unsaturated iron carbonyls and CO, yielding $Fe(CO)_5$. The decomposition yield of $Fe(CO)_5$ in a $SF_6/Fe(CO)_5/CO$ 1:1:6 mixture of 6 Torr total pressure was lower than the yield in the absence of CO. The lower yield in the presence of CO is mostly due to the back-reaction, since CO does not effectively quench IRMP excitation of SF_6. Participation of the back-reaction into decarbonylation processes has been also reported in UV photolyses of metal carbonyls.[22]

(18) Ham, D. O.; Rothschild, M. *Opt. Lett.* **1977**, *1*, 29.
(19) Jones, L. H.; McDowell, R. S.; Goldblatt, M.; Swanson, B. I. *J. Chem. Phys.* **1972**, *57*, 2050.
(20) Clark, R. J. *Inorg. Chem.* **1964**, *3*, 1395.
(21) Langsam, Y.; Ronn, A. M. *J. Chem. Phys.* **1984**, *80*, 749.
(22) Ouderkirk, A. J.; Weitz, E. *J. Chem. Phys.* **1983**, *79*, 1089.

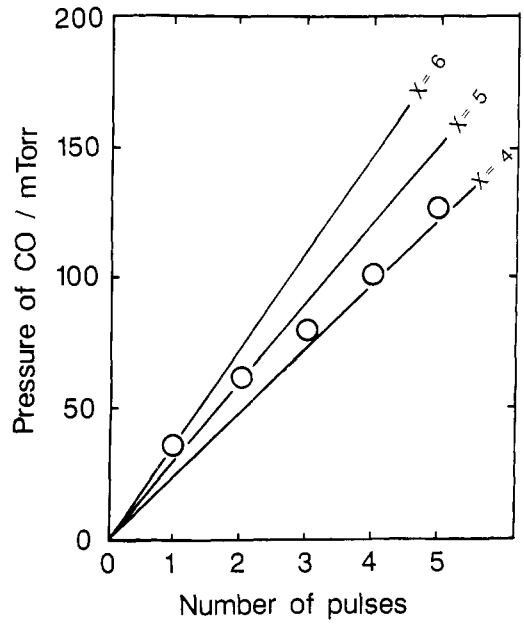

Figure 1. Pressure of CO formed versus number of laser pulses in the TEA CO_2 laser photolysis of SF_6 and $Fe(CO)_5$ mixtures. Pressures of SF_6 and $Fe(CO)_5$ were 0.5 Torr each, and incident laser fluence was 0.163 J cm^{-2}. Three lines were calculated for X = 4, 5, and 6; see text for details.

Trapping of the Intermediate. In order to confirm the primary species of coordinatively unsaturated iron carbonyls, a mixture of SF_6 (0.5 Torr) and $Fe(CO)_5$ (0.2 Torr) was irradiated in the presence of excess PF_3 (10 Torr). Yardley and co-workers have shown that PF_3 can be used as a trapping reagent to determine the initial distribution of coordinatively unsaturated species produced by photolysis of $Fe(CO)_5$ with a KrF laser.[23] The bond strengths of CO and PF_3 to the transition metals are comparable, and addition to PF_3 to the coordinatively unsaturated species results in easily observable PF_3 complexes. If decarbonylation of the first CO is the slowest and rate-determining step, the initially formed $Fe(CO)_4$ will either decompose rapidly into Fe via sequential decarbonylation or be trapped by PF_3 once the gas cools. These two processes of $Fe(CO)_4$ compete depending upon the temperature and reaction time.

In fact, $Fe(CO)_4(PF_3)$ was detected as a dominant product at lower conversions (Figure 5), while $Fe(CO)_3(PF_3)_2$, $Fe(CO)_2(PF_3)_3$, $Fe(CO)(PF_3)_4$, or $Fe(PF_3)_5$ were not detected. This result clearly shows that the initial decomposition is the dissociation of one CO from $Fe(CO)_5$, $Fe(CO)_4$ is relatively long-lived, and the rate-determining step is the first decarbonylation from $Fe(CO)_5$ into $Fe(CO)_4$ plus CO.

Mechanism. SF_6-sensitized pyrolyses of many compounds using a CW CO_2 laser have been reported by several groups.[10,24-26] IRMPD and IRMP excitation of SF_6 are well established by using an intense pulsed CO_2 laser,[14-18] and V–V energy transfer between vibrationally excited SF_6 and relatively small molecules such as NO + O_3 and N_2O have been studied.[27,28] On the other hand, the SF_6-sensitized reaction mechanism involving decomposition of relatively large molecules has not been investigated in detail.

Smith and co-workers have reported that SF_6-sensitized decomposition of $Fe(CO)_5$ caused by irradiation of a TEA CO_2 laser follows thermal kinetics.[11,12] Lifetimes for the V–V and V–T/R processes are reported to be 1.1 and 122 μs Torr in SF_6[29,30] and 2.1 and 74 μs Torr in $Fe(CO)_5$,[21] respectively. Collisional V–V and V–T/R processes within SF_6 or $Fe(CO)_5$ may occur with the same order of lifetimes in a mixture of SF_6 and $Fe(CO)_5$. Therefore, decomposition of $Fe(CO)_5$ will proceed after thermal equilibrium is attained in SF_6 via collisional V–V and V–T/R processes. In other words, SF_6-sensitized decomposition of $Fe(CO)_5$ is fundamentally equal to laser flash pyrolysis. Consequently, the reaction temperature in the irradiated volume is an important factor in determining the decomposition rate.

Scheme I[a]

$$SF_6 + nh\nu \rightarrow SF_6^{\ddagger} \text{ (at room temperature)} \quad (3)$$

$$SF_6^{\ddagger} + M \rightarrow SF_6^{*} + M^{*} \quad (4)$$
(thermalization of all gaseous species to a high local temperature)

$$Fe(CO)_5 \xrightarrow{M^*} Fe(CO)_5^{*} \rightarrow Fe(CO)_4 + CO \quad (5)$$
(unimolecular dissociation)

$$Fe(CO)_4 \xrightarrow{M^*} Fe(CO)_3 + CO, \text{ etc.} \quad (6)$$
(sequential dissociation)

(reaction quenched by reverse recombination and cooling)

[a] M = SF_6, $Fe(CO)_5$; ‡ and * denote vibrational and thermal excitation, respectively.

Following irradiation of each laser pulse, a fine mist of small iron particles could be seen visually in the gas. Moreover, the stoichiometry showed that $Fe(CO)_5$ decomposed into Fe + 5CO shot by shot. Therefore, $Fe(CO)_5$ must lose its remaining CO ligands rapidly after the initial decomposition step. This is in accord with a higher temperature shock-tube study of $Fe(CO)_5$ decomposition, which was used to study iron atom nucleation.[31]

On the basis of our results, the following decomposition mechanism (Scheme I) is suggested: IRMP absorption of SF_6 via the ν_3 mode to yield a vibrationally excited SF_6 (eq 3), thermalization of all gaseous species to high local temperature via fast V–V and V–T/R energy transfer (eq 4 and 5), the first decarbonylation in $Fe(CO)_5$ as the rate-determining step by thermal excitation of $Fe(CO)_5$ over the Fe–CO bond dissociation energy (eq 5), and the sequential dissociation of $Fe(CO)_{5-x}$ (x = 1–4) (eq 6) to the iron atom. Finally a nucleation process of iron atoms occurs to yield ultrafine particles of metallic iron. A reverse recombination reaction between $Fe(CO)_{5-x}$ (x = 1–4) and CO is also involved in each decarbonylation step. The decomposition is quenched by temperature cooling via thermal conduction to the gas mixture in the nonirradiated volume. Since dissociation of one Fe–CO bond in $Fe(CO)_5$ is the rate-determining step, the sequential decarbonylations occur thermally once $Fe(CO)_4$ is formed until the gas mixture cools by thermal conduction and diffusion. Back-reactions between coordinatively unsaturated iron carbonyls and CO occur probably with propagation of the decomposition, as shown in Figure 1, but are not important at low conversion because of low CO concentration.

Effect of Irradiation Conditions. In the SF_6-sensitized IR photodecomposition of $Fe(CO)_5$ using a mixture of SF_6 (0.5 Torr) and $Fe(CO)_5$ (0.5 Torr), the decomposition yield was found to be 9.8% at 0.14 J cm^{-2} laser fluence after irradiation of 100 pulses. The decomposition yield increased with the increase of the number of pulses, laser fluence, and SF_6 pressure. Obviously variation of the laser irradiation parameters changed the decomposition yield. Therefore, we measured the consumption of $Fe(CO)_5$ by IR spectroscopy as a function of the number of pulses, laser fluence, pressure of SF_6 and $Fe(CO)_5$, and additives. By way of comparison, the gas chromatographic experiments were carried out to measure the consumption of $Fe(CO)_5$. The ratio of CO

(23) Yardley, J. T.; Gitlin, G.; Nathanson, G.; Rosan, A. M. *J. Chem. Phys.* **1981**, *74*, 370.
(24) Freeman, M. P.; Travis, D. N.; Goodman, M. F. *J. Chem. Phys.* **1974**, *60*, 231.
(25) Shaub, W. M.; Bauer, S. H. *Int. J. Chem. Kinet.* **1975**, *7*, 509.
(26) Riley, C.; Shatas, R. *J. Phys. Chem.* **1979**, *83*, 1679.
(27) Bar-Ziv, E.; Gordon, R. J. *Chem. Phys. Lett.* **1977**, *52*, 355.
(28) Fakhr, A.; Bates, R. D., Jr. *Chem. Phys. Lett.* **1980**, *71*, 381.
(29) Bates, R. D., Jr.; Knudtson, J. T.; Flynn, G. W.; Ronn, A. M. *Chem. Phys. Lett.* **1971**, *8*, 103.
(30) Steinfeld, J. I.; Burak, L.; Sutton, D. G.; Nowak, A. V. *J. Chem. Phys.* **1970**, *52*, 5421.
(31) Frurip, D. J.; Bauer, S. H. *J. Phys. Chem.* **1977**, *81*, 1001.

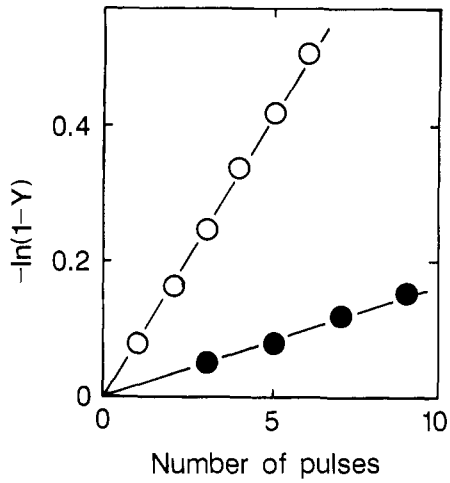

Figure 2. Plot of $-\ln(1 - Y)$ versus number of laser pulses where Y = [consumed $Fe(CO)_5$]/[initial $Fe(CO)_5$] in the absence (open circle) and presence (solid circle) of additive CO (0.5 Torr). Pressures of SF_6 and $Fe(CO)_5$ were 0.5 and 0.2 Torr, respectively, and the incident laser fluence was 0.15 J cm^{-2}.

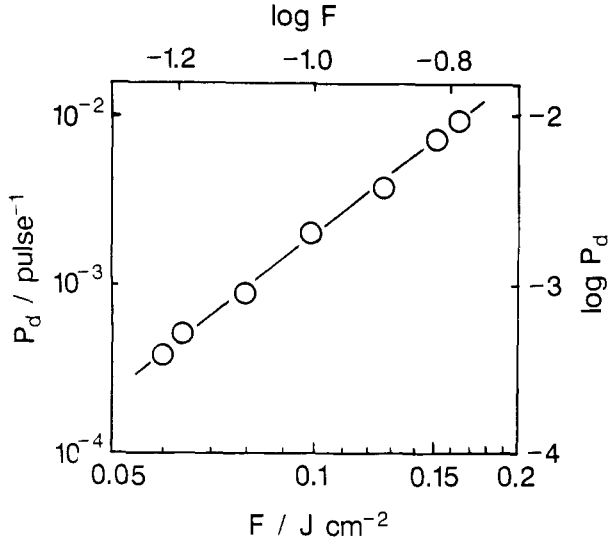

Figure 3. Dependence of incident laser fluence (F) on the decomposition probability (P_d). Pressures of SF_6 and $Fe(CO)_5$ were 0.5 and 0.2 Torr, respectively.

to the consumed $Fe(CO)_5$, 4.7 ± 0.3, was hardly affected by these different irradiation conditions. Hence the stoichiometry follows eq 1 in all the experiments.

A plot of $-\ln(1 - Y)$ versus number of laser pulses gives a straight line at low conversion as shown in Figure 2, where Y = [consumed $Fe(CO)_5$]/[initial $Fe(CO)_5$]. This result shows that the decomposition practically follows first-order kinetics. Therefore, a fractional yield of the decomposition (k_d) is determined to be $k_d = 0.083$ pulse^{-1} from the slope of the line. The decomposition probability (P_d) is given by $P_d = k_d V_{cell}/V_{irr}$, i.e., $P_d = 0.52$ pulse^{-1} under standard irradiation conditions (0.2 Torr of SF_6, 0.5 Torr of $Fe(CO)_5$, and 0.24 J cm^{-2} of laser fluence), where the irradiated volume (V_{irr}) is 7.9 cm^3. With increasing laser fluence (F), P_d increases with a relationship of $P_d \propto F^{6.5}$ obtained from the slope of a log–log plot of P_d versus F as shown in Figure 3. The pressure dependence was studied in the region of 0.1–1.0 Torr of SF_6 and 0.05–1.0 Torr of $Fe(CO)_5$. There were two different pressure regimes, i.e., below and above 0.8 Torr of SF_6 as shown in Figure 4. The increase of SF_6 pressure up to 0.8 Torr increased P_d. In contrast, P_d was nearly unity at SF_6 pressure over 0.8 Torr. When the $Fe(CO)_5$ pressure increased from 0.05 to 1.0 Torr at constant SF_6 pressure of 0.5 Torr, P_d slightly increased from 0.52 to 0.70. With addition of Ar as an inert gas P_d decreased appreciably. For example, P_d at 7 Torr of Ar dropped to 2% of its initial value. Similarly P_d was 0.10

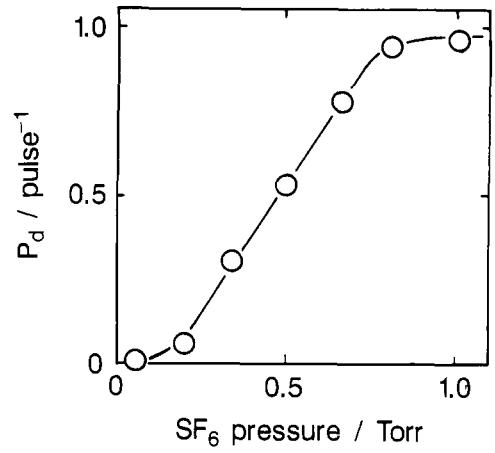

Figure 4. Dependence of SF_6 pressure on P_d. The pressure of $Fe(CO)_5$ was 0.2 Torr, and incident laser fluence was 0.15 J cm^{-2}.

pulse^{-1}, 20% of its initial value, in the presence of 0.5 Torr of CO (Figure 2), and decreased when the pressure of additive CO increased. The quenching efficiency of CO is about 1.5 times higher than that of Ar.

Appreciable variations of P_d by changing the irradiation parameters are qualitatively explained by changes of reaction temperature in irradiated volume, resulting in changes of the number of $Fe(CO)_5$ molecules excited over the dissociation threshold. An increase of fluence (F) and SF_6 pressure leads to an increase in the number of SF_6 molecules in high vibrational levels, resulting in higher reaction temperatures. The effect of Ar on P_d is due to collisional deactivation of reactive $Fe(CO)_5$ molecules. On the other hand, the effect of CO suggests not only collisional deactivation but also the involvement of a back-reaction between coordinatively unsaturated iron carbonyl species and CO as discussed above.

Comparison. Smith and co-workers reported that there was no evidence of the formation of $Fe(CO)_{5-x}(PF_3)_x$ when a mixture of SF_6 (3.0 Torr), $Fe(CO)_5$ (<0.1 Torr), PF_3 (ca. 3 Torr), temperature monitoring gas (0.1 Torr), and N_2 (97 Torr) was irradiated with 1 J cm^{-2} laser fluence.[12] They reported that $Fe(CO)_4$ decomposed very efficiently once the first Fe–CO bond broke, and therefore coordinatively unsaturated fragments trapped by PF_3 were not detected. Consequently they concluded that the first decarbonylation was the slowest and rate-determining step and no intermediates survived under the experimental condition. We assume that they could not detect any trapped products because of relatively higher laser fluence (1 J cm^{-2}), compared to the one (ca. 0.2 J cm^{-2}) used in our experiment. Obviously reaction temperature in the irradiated volume plays a dominant role in determining the branching ratio between the sequential decarbonylation of $Fe(CO)_4$ and the trapping of $Fe(CO)_4$ by PF_3. The sequential decarbonylation proceeds faster at higher temperature. The reaction temperature is estimated to be 3440 and 1140 K at 1 and 0.2 J cm^{-2} laser fluence, respectively, for a mixture of SF_6 (1.0 Torr) and $Fe(CO)_5$ (1.0 Torr), according to our measurement of absorption energy in the mixture which will be reported separately.[32] Although Smith and co-workers used temperature monitoring gas and N_2 in addition to SF_6, $Fe(CO)_5$, and PF_3, only the SF_6–$Fe(CO)_5$–PF_3 mixture was used in the present study. We believe that both experimental results are correct and that the difference results simply from the higher laser fluence and higher pressure of SF_6 used in their work.

The dissociation energy of the Fe–CO bond was first reported to be 55, 5, 32, 23, and 23 kcal mol^{-1} for the series of $Fe(CO)_5$, $Fe(CO)_4$, $Fe(CO)_3$, $Fe(CO)_2$, and Fe(CO), respectively.[33] Recently Lewis et al. reported a more accurate value of 41.5 kcal mol^{-1} for the Fe–CO bond energy of $Fe(CO)_5$.[12] Since the total

(32) Majima, T.; Matsumoto, Y.; Takami, M., to be published.
(33) Engelking, P. C.; Lineberger, W. C. *J. Am. Chem. Soc.* **1979**, *101*, 5569.

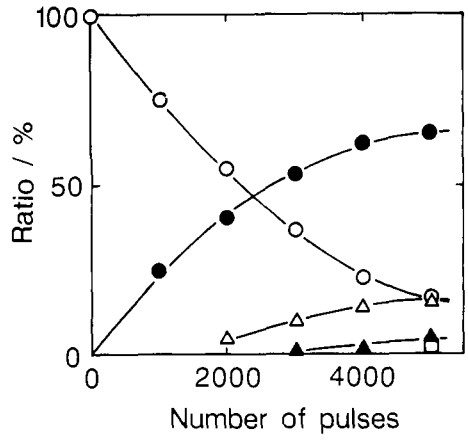

Figure 5. Relative ratios of $Fe(CO)_5$ (open circle) and $Fe(CO)_{5-x}(PF_3)_x$, where x = 1 (solid circle), 2 (open circle), 3 (solid triangle), and 4 (open square) versus number of laser pulses. Pressures of SF_6, $Fe(CO)_5$, and PF_3 were 0.5, 0.2, and 10 Torr, respectively, and incident laser fluence was 0.25 J cm^{-2}.

energy required for $Fe(CO)_5 \rightarrow Fe + 5CO$ (eq 1) is 140 kcal mol^{-1},[34] the Fe–CO bond energy of $Fe(CO)_4$ is corrected to be 20 kcal mol^{-1} as reported by Hepburn and his co-workers.[35] The formation of $Fe(CO)_4(PF_3)$ in the present work is consistent with the revised dissociation energy of the Fe–CO bond in $Fe(CO)_4$ because, if the energy is only 5 kcal mol^{-1}, $Fe(CO)_4$ would decompose rapidly without being trapped by PF_3 at a temperature high enough for dissociation of $Fe(CO)_5$.

Recently IRMPD of $Fe(CO)_5$ at 5 and 16 μm has been studied using a frequency-doubled TEA CO_2 laser[8] and an IR p-H_2 Raman laser.[9] The decomposition of $Fe(CO)_5$ into metallic iron and CO with a ratio of [CO]:[consumed $Fe(CO)_5$] = 5:1 in either experiment is explained by the fast sequential decarbonylation of $Fe(CO)_5$ in highly excited vibrational states. In UV photolysis of $Fe(CO)_5$ sequential decarbonylations occur via vibrationally hot $Fe(CO)_4$ as an unstable intermediate to form $Fe(CO)_3$, $Fe(CO)_2$, Fe(CO), and CO with an RRKM-type statistical dissociation as reported by Hepburn and his co-workers.[35] However, the nascent CO formed by the bond cleavage reaction in UV photolyses has a low degree of internal excitation.[23] Therefore, CO does not remove the excess energy from $Fe(CO)_5$. As a consequence, fast sequential decarbonylation proceeds in the UV photolysis of $Fe(CO)_5$ because of a high degree of the retention of internal excitation energy in the intermediate $Fe(CO)_{5-x}$.[22,23,35,36] In contrast to IRMPD and UV photolysis of $Fe(CO)_5$, in which reactive molecules are produced by direct excitation, SF_6-sensitized decomposition of $Fe(CO)_5$ proceeds thermally via collisional energy transfer processes. The sequential decarbonylation will be slower in SF_6-sensitized decomposition since the energies for decarbonylation of $Fe(CO)_{5-x}$ are supplied by collisions.

CO–Ligand Exchange by PF_3. When a mixture of SF_6, $Fe(CO)_5$, and PF_3 was irradiated, $Fe(CO)_3(PF_3)_2$, $Fe(CO)_2(PF_3)_3$, and $Fe(CO)(PF_3)_4$ were also formed progressively as the number of laser pulses increased (Figure 5). $Fe(CO)_4(PF_3)$ is formed initially as a dominant product (eq 7), loses CO ligand via thermal excitation (eq 8 and 9), and then trapped by PF_3 to yield $Fe(CO)_3(PF_3)_2$ (eq 10). The higher PF_3-substituted iron complexes are formed similarly (eq 8–10 in Scheme II). Trapping of $Fe(CO)_{4-x}(PF_3)_x$ by PF_3 competes with further decarbonylation into $Fe(CO)_{3-x}(PF_3)_x$ and carbonylation by free CO into $Fe(CO)_{5-x}(PF_3)_x$ because of the comparable strengths of the Fe–CO and Fe–PF_3 bonds. Decarbonylation of $Fe(CO)_{5-x}(PF_3)_x$ also competes with dissociation of PF_3 into $Fe(CO)_{5-x}(PF_3)_{x-1}$, which is followed by further decarbonylation into $Fe(CO)_{4-x}(PF_3)_{x-1}$ or trapping either PF_3 back to $Fe(CO)_{5-x}(PF_3)_x$ or by CO into $Fe(CO)_{4-x}(PF_3)_{x-1}$. The CO–ligand exchange reaction by PF_3 occurs step by step depending upon consumption of $Fe(CO)_5$ and the ratio of CO and PF_3 in the reaction mixture. Finally all the CO ligands are probably exchanged by PF_3 to yield $Fe(PF_3)_5$, although $Fe(PF_3)_5$ was not detected because of its low volatility and low sensitivity to gas chromatographic detection. In fact, $Fe(CO)_3(PF_3)_2$ was formed by irradiation of a mixture of SF_6 (0.5 Torr), $Fe(CO)_4(PF_3)$ (0.2 Torr), and PF_3 (10 Torr). Therefore, the CO–ligand exchange reaction by PF_3 is a photosensitized reaction by SF_6 (Schemes I and II).

Scheme II[a]

$$Fe(CO)_4 + PF_3 \rightarrow Fe(CO)_4(PF_3) \quad (7)$$

$$Fe(CO)_{5-x}(PF_3)_x + M^* \rightarrow Fe(CO)_{5-x}(PF_3)_x^* + M \quad (8)$$

$$Fe(CO)_{5-x}(PF_3)_x^* \rightarrow Fe(CO)_{4-x}(PF_3)_x + CO \quad (9)$$

$$Fe(CO)_{4-x}(PF_3)_x + PF_3 \rightarrow Fe(CO)_{4-x}(PF_3)_{x+1} \quad (10)$$

[a] M = SF_6, $Fe(CO)_5$, and PF_3; x = 0, 1, 2, 3, and 4; * denotes thermal excitation.

Black Solid. A black solid sample deposited on a Cu substrate was prepared by irradiation of a mixture of SF_6 (1.0 Torr) and $Fe(CO)_5$ (1.0 Torr) at a laser fluence of 0.23–0.29 J cm^{-2}. SEM and TEM photographs of the solid show the existence of very fine particles. The distribution of the particle size was relatively uniform in the range 65 to 85 Å with the mean particle size being ~80 Å. The black solid turned slightly brown after exposure to air for 3 days and looked like polymeric agglomerations in the SEM photograph.

ICP atomic emission analysis of the solid showed a composition of 86 ± 5 wt % iron. The remaining composition of 14 ± 5 wt % is mostly oxygen as in iron oxides. In X-ray diffractometry, strong diffraction lines at d = 2.087 (111), 1.0809 (200), 1.277 (220), 1.087 (311), 1.041 (222) Å were observed. These are consistent with the face-centered-cubic structure of austenite, (Fe–C)4F, including less than 0.75 wt % carbon. Formation of austenite resulted from primary formation of γ-iron which is usually stable only between 911 and 1392 °C. It is interesting that austenite, which has basically the same structure as γ-iron, is formed as a dominant iron particle in place of α-iron which is stable at lower temperature. Additionally, diffraction lines due to α-iron and iron oxides such as Fe_2O_3 and Fe_3O_4 were observed with low intensities. From these results together with stoichiometry of the decomposition of $Fe(CO)_5$ described in the previous section, the black solid is reasonably assigned to ultrafine particles of metallic iron with a structure similar to γ-iron. The iron particles are very sensitive to oxygen in air and easily oxidized.

Formation of α-iron in conventional pyrolysis of $Fe(CO)_5$ is well known. The formation of γ-iron in the present work probably resulted from the differences of environmental conditions in the final iron atom nucleation process. Effects of surface and self-catalysis cannot be avoided in conventional pyrolysis. In contrast, SF_6-sensitized IR photodecomposition is free from such heterogeneous effects; the γ-iron particles initially formed in the high-temperature-reaction gas cool down within a very short time scale of 100 ns to few hundreds of microseconds while retaining their structure. The reaction temperature, immediately after a pulse, is estimated to be 900–1200 °C from the absorption energy in the mixture,[30] where γ-iron is predominantly formed in place of α-iron.

In conclusion, the decomposition of $Fe(CO)_5$ proceeds via sequential decarbonylation, being sensitized by SF_6 in the vibrational excited levels in an SF_6–$Fe(CO)_5$ mixture. Trapping of coordinatively unsaturated intermediates by PF_3 indicates that the rate-determining process is the first decarbonylation of excited $Fe(CO)_5$ into $Fe(CO)_4$ and CO. Final products are CO and ultrafine particles of γ-iron, following $Fe(CO)_5 \rightarrow Fe + 5CO$.

The formation of γ-iron in place of α-iron is of particular interest. Fine metallic particles have numerous applications in many technologies. Ultrafine particles of γ-iron observed in the present work may offer possibilities in structural and compositional

(34) Housecraft, C. E.; Wade, K.; Smith, B. C. *J. Organomet. Chem.* **1979**, *170*, C1.
(35) Waller, I. M.; Davis, H. F.; Hepburn, J. W. *J. Phys. Chem.* **1987**, *91*, 506. Waller, I. M.; Hepburn, J. W. *J. Chem. Phys.* **1988**, *88*, 6658.
(36) Majima, T., to be published.

control of fine metal particles. Moreover, this method has many advantages with respect to the experimental conditions, because a parallel laser beam is used for irradiation.

It is also noteworthy that isomerization among *cis*-2-butene, *trans*-2-butene, and 1-butene via cis-trans isomerization and 1,3-hydrogen transfer processes has been observed in a mixture of SF_6-$Fe(CO)_5$-butene irradiated by a TEA CO_2 laser light.[36] In the isomerization reactions the coordinatively unsaturated iron carbonyls act as catalytic species. The generation of a catalytic species from transition metal carbonyls via the SF_6-photosensitized decomposition will be one of the candidates for application of a TEA CO_2 laser to organic syntheses.

Acknowledgment. Thanks are due to Satoru Utsuno, Mitsuhiro Kurokawa, Shigeru Ishikawa, and Tatsuki Kawamura, undergraduate students of Science University of Tokyo in 1984-1988, for their collaboration in the course of the experiments. We are grateful to Yasuhiro Iimura for X-ray diffractometry, and Dr. Tesshu Miyahara and Ryugo Maeda in Dainippon Ink & Chemicals for TEM photographs.

Design of Redox Systems for the Selective Transport of Electrons across Liquid Membranes: Nickel(II,III) Tetraaza Macrocyclic Complexes

Giancarlo De Santis, Michela Di Casa, Mario Mariani, Barbara Seghi, and Luigi Fabbrizzi*

Contribution from the Dipartimento di Chimica Generale, Università di Pavia, 27100 Pavia, Italy.
Received February 22, 1988

Abstract: The complexes $NiLX_2$ (L = *N*-cetylcyclam; X = Cl, ClO_4) have been synthesized to be used as carriers for the transport of electrons across a CH_2Cl_2 bulk liquid membrane, through the Ni^{II}/Ni^{III} redox change. Two-phase (water/dichloromethane) experiments have shown that aqueous peroxydisulfate ion is able to oxidize $Ni^{II}LCl_2$, but not $Ni^{II}L(ClO_4)_2$, due to the very large difference of the $Ni^{III,II}$ redox potentials. On the other hand, the $[Ni^{III}LCl_2]Cl$ complex in the organic layer can be reduced by a series of aqueous cationic reducing agents, according to a rate sequence ($Ti^{III} > Cr^{II} > Fe^{II} > [Co^{II}$ cage] complex) that does not correlate with their redox potential values. The anionic reducing agent I^- does not reduce $[Ni^{III}LCl_2]Cl$ under two-phase conditions, whereas it does in homogeneous conditions. Three-phase experiments have been performed in which electrons are transported from an aqueous reducing phase, containing the metal-centered agents mentioned above, to an aqueous oxidizing phase, containing peroxydisulfate and chloride, across a CH_2Cl_2 membrane containing the $[Ni^{II}LCl_2]/[Ni^{III}LCl_2]Cl$ redox couple. A counterflow of Cl^- anions is coupled to the flow of electrons. Under the conditions employed, the electron transport is complete in a time ranging from minutes (reducing agent, Ti^{III}) to several hours ([Co^{II} cage] complex).

A liquid membrane is a water-immiscible organic layer (bulk or supported on a microporous film) that separates two aqueous layers. Experiments on the transport of chemical entities across bulk or supported liquid membranes have been designed by many researchers in the past decade, with the aim being to mimic and rationalize biological processes and also because of important practical applications. Much of the work has been devoted to the transport of metal ions,[1] mainly of the s block, and involved the design of appropriate carriers able to complex in a selective way the cation in the liquid membrane. On the other hand, in spite of the fundamental role of redox active membranes in biology, very few studies have been reported on the transport of electrons across liquid membranes. The above studies have considered as electron carriers classical metal complexes, like ferrocene[2] and nickel bisdithiolene,[3] or organic substrates, like quinones,[2,4,5] whereas charge neutrality in the membrane was ensured through the simultaneous flow of anions, cations, or protons. In these studies attention has been centered on the design of the electron-transport experiment, to be coupled to a flow of cations or to a counterflow of anions, and on the control of the transport by a concentration gradient (eventually photochemically generated).[2,5]

In the present work we were interested in designing a redox system, to be used as an electron carrier, whose redox potential could be controlled, in order to perform the *selective* transport of electrons from an electron source phase (ESP) to an electron receiving phase (ERP). In a selective transport, the carrier should be able to discriminate among a mixture of reducing agents in ESP and/or a mixture of oxidizing agents in ERP.

As a potentially modulable electron carrier, we have used a system based on the Ni^{II} and Ni^{III} complexes of the novel tetraaza macrocycle *N*-cetylcyclam (**1**, L). It is well documented that

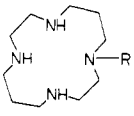

R = $C_{16}H_{33}$ **1**

R = H **2**

encircling of nickel(II) by the precursor tetraaza macrocycle cyclam (**2**) permits easy attainment, in solution of polar solvents (H_2O, MeCN, DMSO), of the otherwise unstable trivalent state whose chemistry has been extensively investigated in the past years.[6] Appending a C_{16} aliphatic chain on the cyclam framework makes the nickel(II,III) complexes soluble in apolar and poorly polar solvents, immiscible with water, to be used as a liquid membrane. Since these solvents have no coordinating ability, the

(1) Izatt, S. R.; Hawkins, R. T.; Christensen, J. J.; Izatt, R. M. *J. Am. Chem. Soc.* **1985**, *107*, 63-68. Di Casa, M.; Fabbrizzi, L.; Perotti, A.; Poggi, A.; Riscassi, R. *Inorg. Chem.* **1986**, *25*, 3984-3987, and references therein.
(2) Grimaldi, J. J.; Boileau, S.; Lehn, J. M. *Nature (London)* **1977**, *265*, 229-330.
(3) Grimaldi, J. J.; Lehn, J. M. *J. Am. Chem. Soc.* **1979**, *101*, 1333-1334.
(4) Danesi, P. R. *J. Membr. Sci.* **1986**, *29*, 287-293.
(5) Jackman, D. C.; Thomas, C. A.; Rillema, D. P.; Callahan, R. W.; Yan, S.-L. *J. Membr. Sci.* **1987**, *30*, 213-225.
(6) Fabbrizzi, L. *Comments Inorg. Chem.* **1985**, *4*, 33-54, and references therein.

0002-7863/89/1511-2422$01.50/0